

Hyperfine-Structure-Induced Purely Long-Range Molecules

Katsunari Enomoto,¹ Masaaki Kitagawa,¹ Satoshi Tojo,² and Yoshiro Takahashi^{1,3}

¹*Department of Physics, Graduate School of Science, Kyoto University, Kyoto 606-8502, Japan*

²*Department of Physics, Faculty of Science, Gakushuin University, Tokyo 171-8588, Japan*

³*CREST, Japan Science and Technology Agency, Kawaguchi, Saitama 332-0012, Japan*

(Received 18 July 2007; published 24 March 2008)

We have experimentally observed and theoretically identified a novel class of purely long-range molecules. This novel purely long-range state is formed due to a very weak hyperfine interaction that is usually treated only as a small perturbation in molecular spectra. Photoassociation spectroscopy of ultracold ytterbium (^{171}Yb) atoms with the $^1S_0\text{-}^3P_1$ intercombination transition presents clear identification of molecular states and the shallowest molecular potential depth of about 750 MHz among the purely long-range molecules ever observed.

DOI: [10.1103/PhysRevLett.100.123001](https://doi.org/10.1103/PhysRevLett.100.123001)

PACS numbers: 33.15.Pw, 34.20.Cf, 37.10.De

Photoassociation (PA) spectroscopy of ultracold atoms has become a powerful tool for the investigation of so-called long-range molecules with the classical outer turning points of several to hundreds of nanometers [1]. In the long-range molecules, properties of the molecular states are closely related to properties of their constituent atoms. A special class of long-range molecules is called a purely long-range (PLR) molecule. It has a classical inner turning point at a long internuclear distance where the short-range interaction due to the overlap of atomic electron clouds is negligible. Therefore, rovibrational levels of the PLR states are precisely calculated without information of the unknown short-range interaction.

The possibility of observing the bound levels in PLR molecules was already discussed about 30 years ago [2,3], and the development of laser cooling techniques has at last enabled the experimental observations of the PLR states for alkali-metal atoms [4–9] and metastable helium [10] with PA spectroscopy. For these atoms the PLR molecules are formed due to the interplay between a resonant dipole interaction and a spin-orbit interaction. The spin-orbit coupling causes an avoided crossing between attractive and repulsive potentials correlating to different asymptotes of the fine structure, and this results in the formation of the potential minimum at a long internuclear distance r . The potential curves of the PLR states are shown in Fig. 1. PA spectroscopic studies of these states have been performed to verify a retardation effect [11] and to precisely determine radiative lifetimes.

A similar avoided crossing occurs due to a hyperfine interaction. Although the hyperfine interaction is usually treated only as a small perturbation in molecular spectra, it plays an important role in the PA spectroscopy probing near the dissociation limit [12–15]. It is possible at a very long r that the total electronic angular momentum J_a is much more strongly coupled with the nuclear spin than with the internuclear axis. This coupling order of angular momenta is different from that of the usual Hund's case (c), where the coupling between J_a and the molecular axis is

much stronger than the hyperfine interaction. The coupling scheme changes from this unusual one to the usual Hund's case (c) with decreasing r . In the transient region, PLR states are expected to be formed due to the interplay between the hyperfine interaction and the resonant dipole interaction. However, such states have not been experimentally observed so far, since the hyperfine splittings of alkali-metal atoms are small and it is difficult to resolve resonance lines locating within several hundreds of megahertz from the dissociation limit for the dipole-allowed PA transitions with large natural linewidths. It should be noted that molecular states in which the hyperfine splitting is much larger than the binding energies have been normally studied for the electronic ground $S + S$ asymptotes of alkali-metal atoms. The van der Waals interaction for these molecules is replaced with the resonant dipole interaction in the present case. Since the resonant dipole interaction can be both repulsive and attractive, being different from the attractive van der Waals interaction, the PLR states are formed in the present case.

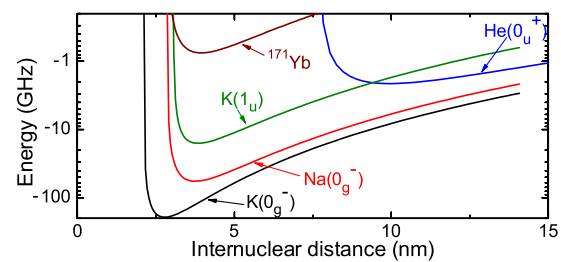


FIG. 1 (color online). Potentials for PLR states of various atoms. The potential curves for alkali-metal atoms correlate to the $^2S_{1/2} + ^2P_{3/2}$ atomic states, and that for helium correlates to the $^3S_1 + ^3P_0$ state. Except ^{171}Yb , only the resonant dipole interaction and the fine-structure splitting are taken into account to calculate these potentials. The potentials of heavy alkali-metal atoms (Cs, Rb), which are not shown here, have deeper wells than those of K and Na.

In this Letter, we report the first experimental observation of this hyperfine-structure-induced PLR state by carrying out high-resolution PA spectroscopy of a fermionic isotope ^{171}Yb with the 1S_0 - 3P_1 intercombination transition. Using the intercombination lines, one can resolve rovibrational levels very close, even about 1 MHz, to the dissociation limit [16,17]. The molecular potential depth is about 750 MHz, which is shallowest among the PLR molecules ever observed as shown in Fig. 1. We have also observed other states lying within 1 GHz of the dissociation limit, and have assigned all the PA resonances by considering the rovibrational level structure and changing the temperature of atomic clouds. These results in this Letter provide a foundation for many applications of ultracold ^{171}Yb atoms. Efficient optical control of a scattering length is expected for the use of the intercombination transition [18]. Based partly on this work, two-color PA spectroscopy has recently been performed to precisely determine the ground-state C_6 potential coefficient and the scattering lengths of all isotopic combinations [19].

At long r the interatomic interaction can be treated as a perturbation and the molecular state is well represented by products of atomic states (Movre-Pichler model). An atom pair in the electronic ground state is expressed as

$$|g\rangle = |(^1S_0)_1\rangle |(^1S_0)_2\rangle |I_g, \Phi_g\rangle_{\text{nucl}}, \quad (1)$$

where subscripts 1 and 2 refer to the atoms and $|I_g, \Phi_g\rangle_{\text{nucl}}$ represents the wave function of the nuclear spins with Φ_g the axial projection of the total nuclear spin I_g . ^{171}Yb has a nuclear spin $i = 1/2$, and thus s - and p -wave collisions occur for $I_g = 0$ and 1, respectively, due to the antisymmetry of the total wave function. Since all of the observed spectra are identified to the transitions from the s - and p -wave scattering states as described later, we do not consider the other higher partial-wave states. The electronic excited states are also written as

$$|\alpha\rangle = \frac{|(^3P_1)f, \phi\rangle_1 |(^1S_0)\eta\rangle_2 + |(^1S_0)\eta\rangle_1 |(^3P_1)f, \phi\rangle_2}{\sqrt{2}}, \quad (2)$$

$$|\beta\rangle = \frac{|(^3P_1)f, \phi\rangle_1 |(^1S_0)\eta\rangle_2 - |(^1S_0)\eta\rangle_1 |(^3P_1)f, \phi\rangle_2}{\sqrt{2}}, \quad (3)$$

where ϕ is the projection of the atomic total angular momentum f onto the molecular axis for the 3P_1 state, and η is the projection of the nuclear spin i for the 1S_0 state. Here we classify these states into two sets, $|\alpha\rangle$ and $|\beta\rangle$, which are symmetric and antisymmetric for the exchange of atoms, respectively.

Adiabatic potentials of $^{171}\text{Yb}_2$ correlating to the $^1S_0 + ^3P_1$ atomic state are obtained by diagonalization of the following Hamiltonian:

$$H = \frac{\mathbf{d}_1 \cdot \mathbf{d}_2 - 3d_{1z}d_{2z}}{r^3} + a(\mathbf{i}_1 \cdot \mathbf{j}_1 + \mathbf{i}_2 \cdot \mathbf{j}_2) + V_{\text{vdW}}(r), \quad (4)$$

where $a = 3957$ MHz is the atomic hyperfine coupling constant [20], and \mathbf{d}_k , d_{kz} , \mathbf{i}_k , and \mathbf{j}_k are the transition dipole moment, the axial component of \mathbf{d}_k , the nuclear spin, and the electronic total angular momentum of the atom k ($k = 1, 2$), respectively. The value of the transition dipole moment is 0.311 a.u., which is calculated from the radiative lifetime of 874 ns for the 3P_1 state [21]. Since the 3P_2 and 3P_0 states are energetically separated more than 700 cm^{-1} from the 3P_1 state, the mixing of these states is negligible. $V_{\text{vdW}}(r)$ represents the van der Waals interaction. Since this interaction is much weaker than the other interactions in the interested range of r , we adopt an approximation that it is given by $-C_{6e}/r^6$ with only one parameter C_{6e} , which is later used for a fit of the observations. Higher order dispersion terms are negligibly small in the range $r \geq 3$ nm. The potential matrix from Eq. (4) is diagonalized at fixed internuclear separations, and this result is shown in Fig. 2. Since the interaction given by Eq. (4) does not couple the basis sets $|\alpha\rangle$ and $|\beta\rangle$, the potentials are accordingly classified into two groups. The axial projection Φ_e of the angular momentum $\mathbf{F} = \mathbf{j}_1 + \mathbf{j}_2 + \mathbf{i}_1 + \mathbf{i}_2$, namely $\Phi_e = \phi + \eta$, is a good quantum number. Note that the axial projection Ω of \mathbf{J}_a is not a good quantum number at all. The selection rule of the PA transition is understood by considering the nonrotating states. The molecular transition dipole moment $\mathbf{d}_1 + \mathbf{d}_2$ does not couple $|\alpha\rangle$ to $|g\rangle$ of $I_g = 0$, and does not couple $|\beta\rangle$ to $|g\rangle$ of $I_g = 1$. Therefore, the electronic excited states constructed from the basis sets $|\alpha\rangle$ and $|\beta\rangle$ are optically accessible only from the p - and s -wave ground-state scattering states, respectively.

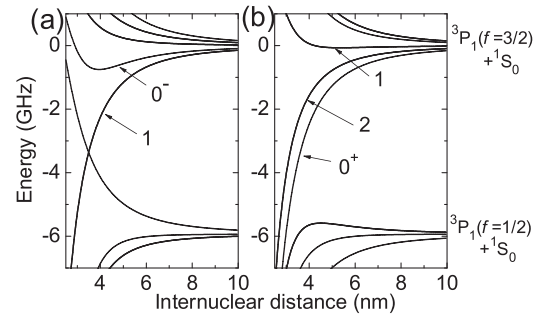


FIG. 2. Adiabatic potentials near the $^1S_0 + ^3P_1$ dissociation limit obtained from Eq. (4). (a),(b) The potentials for the states composed of the basis sets $|\alpha\rangle$ and $|\beta\rangle$, respectively. The nuclear spin i of ^{171}Yb is $1/2$. The value of C_{6e} is set to be 2810 a.u., as discussed later. The potentials are labeled by $|\Phi_e|$, and the \pm superscript indicates the reflection symmetry with respect to a plane containing the molecular axis.

The rotational states of the electronic excited states are specified by the total angular momentum T_e , which is the sum of F and the rotation. Since Φ_e is the projection on the molecular axis of T_e as well as that of F , the condition $T_e \geq \Phi_e$ is imposed. The total angular momentum T_g of the electronic ground state is the sum of I_g and the rotation, and the selection rules are $|T_e - T_g| \leq 1$ and $|\Phi_e - \Phi_g| \leq 1$. For each $\Phi_e = 0$ state only even or odd T_e are allowed, because the wave function of the rotating states has to be antisymmetric for the permutation of the fermionic nuclei of $^{171}\text{Yb}_2$ [22]. For $\Phi_e \neq 0$ states all T_e are allowed, since one of the parity eigenstates ($|T_e, \Phi_e\rangle \pm |T_e, -\Phi_e\rangle$)/ $\sqrt{2}$ fulfills this antisymmetric condition for a given T_e . Comprehensive discussions about the molecular symmetry in the asymptotic region are seen in Refs. [13–15,23], and the hyperfine structure has been analyzed in the region where the binding energies are much larger than the hyperfine splitting and Ω is approximately a good quantum number [12,14,15].

As shown in Fig. 2(a), the 0^- state potential curve supports the PLR state. Other attractive potentials shown in Fig. 2(a) and 2(b) correlating to the $^1S_0 + ^3P_1(f=3/2)$ state are roughly proportional to r^{-3} , and thus the LeRoy-Bernstein formula [24] is helpful for the assignment of the rovibrational levels. The $|\Phi_e| = 2$ state shown in Fig. 2(b) cannot be optically accessed from the electronic ground state, since $\Phi_g = 0$ for the s -wave collision.

We have observed PA spectra at two different temperatures of about $2 \mu\text{K}$ and $25 \mu\text{K}$. Since the C_6 potential coefficient for the electronic ground state is about 2000 a.u. [19,25], the height of the p -wave centrifugal barrier is about $40 \mu\text{K}$. Therefore, it is expected that only the s -wave collision occurs at $2 \mu\text{K}$ and the p -wave collision also becomes probable at $25 \mu\text{K}$. The experimental setup and procedure are similar to our previous experiment for bosonic isotopes [16]. ^{171}Yb atoms are collected in a magneto-optical trap (MOT) and then transferred into a crossed optical far-off resonant trap (FORT). After evaporative cooling of a spin mixture of ^{171}Yb atoms, typically 2×10^4 atoms at $25 \mu\text{K}$ remain in the trap. In order to reach the temperature of $2 \mu\text{K}$, we have performed sympathetic cooling of ^{171}Yb atoms with thermal contact with evaporatively cooled ^{174}Yb atoms. The ^{171}Yb and ^{174}Yb atoms are simultaneously trapped in the MOT and are transferred into the FORT [26]. After the sympathetic cooling, 2×10^4 ^{171}Yb atoms are typically obtained at $2 \mu\text{K}$. Then the PA light is applied to the trapped atoms. We have observed PA signals by measuring the number of the survived atoms with an absorption imaging method using the strong $^1S_0 - ^1P_1$ transition.

Figure 3 shows the obtained PA spectra at $2 \mu\text{K}$. We have observed 8 PA lines up to 1 GHz detuning from the atomic resonance. All these observed lines are assigned to the transitions from the s -wave scattering state to the $T_e = 1$ states of the 0^+ state shown in Fig. 2(b). Note that only

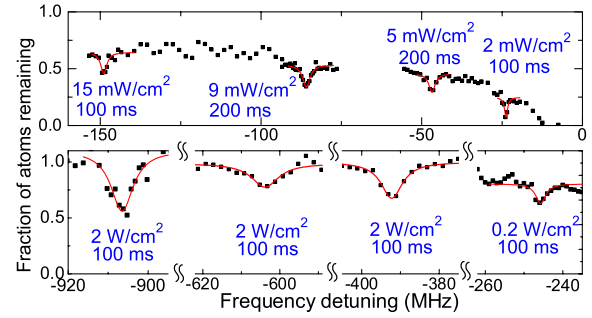


FIG. 3 (color online). PA spectra of ^{171}Yb atoms at $2 \mu\text{K}$. The fraction of atoms remaining is plotted against the detuning from the $^1S_0 + ^3P_1(f=3/2)$ asymptote. The lines are fitted Lorentzian profiles to guide the eye. The labels show the intensities and the duration times of the PA laser.

odd T_e are allowed for this 0^+ state [22] and the s -wave state has uniquely $T_g = 0$. The vibrational progression is well explained by the LeRoy-Bernstein formula [24].

Figure 4 shows the obtained PA spectra at $25 \mu\text{K}$. We have observed 20 PA resonances in this frequency range. In addition to the lines denoted as S observed at $2 \mu\text{K}$, also several lines are observed. The lines denoted as P are assigned to the transitions from the p -wave scattering state to the $|\Phi_e| = 1$ state shown in Fig. 2(a). The total angular momentum quantum numbers T_e for these lines are 1–3, since $T_e \geq |\Phi_e|$ and the p -wave state can have $T_g = 0–2$. Above -400 MHz detuning another series of resonance lines is observed. These four lines denoted as L are assigned to the transitions from the p -wave state to $T_e = 1, 3$ rovibrational states of the 0^- PLR state shown in Fig. 2(a). Only odd T_e are allowed for this state. All the resonance lines observed at $25 \mu\text{K}$ are assigned to the transitions from the s - and p -wave states, and the contribution from the other higher partial-wave states is not recognized. Most of the widths of the atom-loss PA signals for the s -wave state are larger than those for the p -wave state, which might be explained by a larger saturation effect for the PA signals for the s -wave state.

To theoretically reproduce the four observed rovibrational levels of the PLR state, we assume that the interatomic potential $V(r)$ is given by

$$V(r) = V_{\text{plr}}(r) + \frac{\hbar^2[T_e(T_e + 1) + \langle F^2 \rangle - 2\Phi_e^2]}{2\mu r^2}, \quad (5)$$

where $V_{\text{plr}}(r)$ is the potential obtained by the diagonalization of the Hamiltonian (4) and μ is the reduced mass. The expectation value $\langle F^2 \rangle$ of F^2 is calculated at each r . The retardation effect on the resonant dipole interaction is included [27]. The coefficient C_{6e} is the only free parameter for this potential. We have obtained several data of the resonance frequencies for different intensities of the PA laser and the FORT laser at about $15 \mu\text{K}$, and extrapolated the data to the zero intensities of these lasers. The FORT

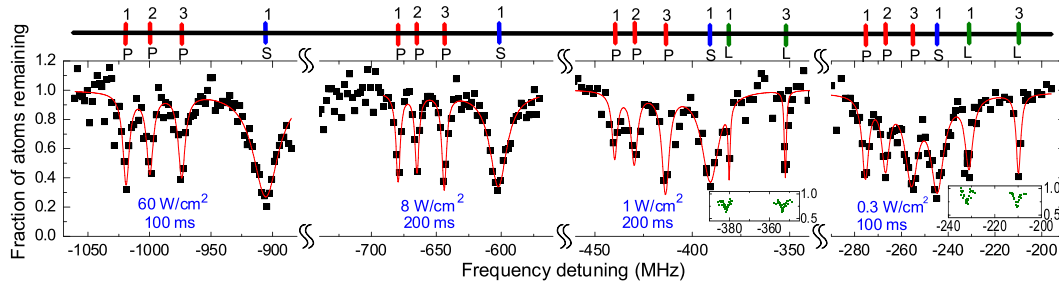


FIG. 4 (color online). PA spectra of ^{171}Yb atoms at $25\ \mu\text{K}$. The fraction of atoms remaining is plotted against the detuning from the $^1S_0 + ^3P_1(f = 3/2)$ asymptote. The lines are fitted Lorentzian profiles to guide the eye. The intensities and the duration times of the PA laser are written below the spectra. The bars above the graph show peak positions of the PA lines. The symbols S , P , and L denote the transitions from the s -wave state, from the p -wave state, and to the PLR state from the p -wave state, respectively. The numbers indicate the values of T_e . The insets show the spectra observed at about $15\ \mu\text{K}$.

laser causes a light shift of about 3 MHz to the blue side. A frequency shift due to the finite temperature is estimated from the numerical result of Ref. [28]. After compensation of these shifts, the rovibrational levels are determined to be $-383.4(1.0)$ MHz ($\nu = 1$, $T_e = 1$), $-355.4(1.0)$ MHz ($\nu = 1$, $T_e = 3$), $-234.0(1.0)$ MHz ($\nu = 2$, $T_e = 1$), and $-212.4(1.0)$ MHz ($\nu = 2$, $T_e = 3$), where ν is the vibrational quantum number. All the four levels are reproduced within the experimental uncertainty when C_{6e} is $2810(30)$ a.u. From this calculation the $\nu = 0$ levels are expected to be found at -595 MHz and -561 MHz. However, the spectral lines for these levels are not recognized. This is probably because the Franck-Condon densities for the transitions to the $\nu = 0$ states are very small. A numerical calculation based on the recent result [19] reveals that the Franck-Condon densities for the $\nu = 0$ states are smaller by about a factor of 100 than those for the $\nu = 1$ states.

In conclusion, we present PA spectroscopy of a fermionic isotope ^{171}Yb for the $^1S_0 - ^3P_1$ intercombination transition. We have successfully observed a novel PLR molecule originating from the hyperfine interaction. The binding energies of the four observed states could be accurately reproduced by the calculation only with the hyperfine constant, the transition dipole moment, and the dispersion parameter C_{6e} . In addition, we have assigned all the observed PA lines.

We thank M. Kumakura, P. S. Julienne, and E. Tiemann for helpful comments. We acknowledge S. Uetake, Y. Takasu, K. Kasa, Y. Nishio, A. Yamaguchi, and T. Fukuhara for their experimental assistance. This work was partially supported by Grant-in-Aid for Scientific Research of JSPS (No. 18043013 and No. 18204035), SCOPE-S, and 21st Century COE ‘‘Center for Diversity and Universality in Physics’’ from MEXT of Japan.

[1] K. M. Jones *et al.*, Rev. Mod. Phys. **78**, 483 (2006).

- [2] M. Movre and G. Pichler, J. Phys. B **10**, 2631 (1977).
 [3] W. C. Stwalley, Y.-H. Uang, and G. Pichler, Phys. Rev. Lett. **41**, 1164 (1978).
 [4] R. A. Cline, J. D. Miller, and D. J. Heinzen, Phys. Rev. Lett. **73**, 632 (1994).
 [5] L. P. Ratliff *et al.*, J. Chem. Phys. **101**, 2638 (1994).
 [6] H. Wang, P. L. Gould, and W. C. Stwalley, Phys. Rev. A **53**, R1216 (1996).
 [7] A. Fioretti *et al.*, Phys. Rev. Lett. **80**, 4402 (1998).
 [8] X. Wang *et al.*, Phys. Rev. A **57**, 4600 (1998).
 [9] D. Comparat *et al.*, Eur. Phys. J. D **11**, 59 (2000).
 [10] J. Léonard *et al.*, Phys. Rev. Lett. **91**, 073203 (2003).
 [11] K. M. Jones *et al.*, Europhys. Lett. **35**, 85 (1996).
 [12] C. J. Williams and P. S. Julienne, J. Chem. Phys. **101**, 2634 (1994).
 [13] E. R. I. Abraham, W. I. McAlexander, H. T. C. Stoof, and R. G. Hulet, Phys. Rev. A **53**, 3092 (1996).
 [14] D. Comparat *et al.*, Eur. Phys. J. D **11**, 59 (2000).
 [15] E. Tiesinga *et al.*, Phys. Rev. A **71**, 052703 (2005).
 [16] S. Tojo *et al.*, Phys. Rev. Lett. **96**, 153201 (2006).
 [17] T. Zelevinsky *et al.*, Phys. Rev. Lett. **96**, 203201 (2006).
 [18] R. Ciurylo, E. Tiesinga, and P. S. Julienne, Phys. Rev. A **71**, 030701(R) (2005).
 [19] M. Kitagawa *et al.*, Phys. Rev. A **77**, 012719 (2008).
 [20] D. L. Clark, M. E. Cage, D. A. Lewis, and G. W. Greenlees, Phys. Rev. A **20**, 239 (1979).
 [21] J. E. Golub, Y. S. Bai, and T. W. Mossberg, Phys. Rev. A **37**, 119 (1988).
 [22] The symmetry property of each state can be derived by combining formalisms about the symmetry of electronic and nuclear-spin wave functions [J. Brown and A. Carrington, *Rotational Spectroscopy of Diatomic Molecules* (Cambridge University Press, Cambridge, England, 2003)]. See also Refs. [13–15, 23].
 [23] B. Gao, Phys. Rev. A **54**, 2022 (1996).
 [24] R. J. LeRoy and R. B. Bernstein, J. Chem. Phys. **52**, 3869 (1970).
 [25] K. Enomoto *et al.*, Phys. Rev. Lett. **98**, 203201 (2007).
 [26] K. Honda *et al.*, Phys. Rev. A **66**, 021401(R) (2002).
 [27] W. J. Meath, J. Chem. Phys. **48**, 227 (1968).
 [28] K. M. Jones, P. D. Lett, E. Tiesinga, and P. S. Julienne, Phys. Rev. A **61**, 012501 (1999).